35th Annual International Conference of the IEEE EMBS
Osaka, Japan, 3 - 7 July, 2013

Real-Time Temperature Control System Based on the Finite Element Method for Liver Radiofrequency Ablation: Effect of the Time Interval on Control

Yosuke Isobe, Hiroki Watanabe, Nozomu Yamazaki, XiaoWei Lu, Yo Kobayashi, Tomoyuki Miyashita, Makoto Hashizume, and Masakatsu G. Fujie, *Fellow, IEEE*

***Abstract*—Radiofrequency (RF) ablation is increasingly being used to treat liver cancer because it is minimally invasive. However, it is difficult for operators to control the size of the coagulation zones precisely, because no method has been established to form an adequate and suitable ablation area. To overcome this limitation, we propose a new system that can control the coagulation zone size. The system operates as follows: 1) the liver temperature is estimated using a temperature-distribution simulator to reduce invasiveness; 2) the output power of the RF generator is controlled automatically according to the liver temperature. To use this system in real time, both the time taken to calculate the temperature in the simulation and the control accuracy are important. We therefore investigated the relationship between the time interval required to change the output voltage and temperature control stability in RF ablation. The results revealed that the proposed method can control the temperature at a point away from the electrode needle to obtain the desired ablation size. It was also shown to be necessary to reduce the time interval when small tumors are cauterized to avoid excessive treatment. In contrast, such high frequency feedback control is not required when large tumors are cauterized.**

I. Introduction

Radiofrequency (RF) ablation, an important method for the treatment of liver tumors, has been increasingly used in recent years. The RF ablation procedure and the coagulation mechanism are shown in Fig. 1. In RF ablation, (1) the tumor is detected by using ultrasonic diagnostics, (2) an electrode needle is inserted into the tumor percutaneously and microwaves are output between the electrode needle and the return electrodes patched on the thighs, (3) the tissue around the electrode needle is heated by ionic agitation generated by the microwaves, and (4) the tissue coagulates when it reaches a temperature of 60°C, and becomes completely necrotic at about 90°C because of moisture evaporation from the liver tissue. Therefore, this percutaneous procedure is a minimally invasive therapy and provides effective and safe treatment for liver cancer patients.

Manuscript received February 5, 2013. This work was supported in part by the Global COE (Centers of Excellence) Program "Global Robot Academia," in part by a Grant for Scientific Research (B) (22360108), and by a Grant for Scientific Research (A) (23240081) from MEXT.

Y. Isobe and XW. Lu are Members of the Graduate School of Science and Engineering, Waseda University, Japan. (59-309, 3-4-1 Okubo, Shinjuku Ward, Tokyo, Japan. Corresponding author: phone: +81-3-5286-3412; fax: +81-3-5291-8269; e-mail: i3s.1o415@ruri.waseda.jp).

H. Watanabe, N. Yamazaki, Y. Kobayashi, T. Miyashita, and M. G. Fujie are Members of the Faculty of Science and Engineering, Graduate School of Science and Engineering, Waseda University, Japan.

M. Hashizume is a Member of the Center for the Integration of Advanced Medicine and Innovative Technology, Kyushu University Hospital, Japan.

A. Practical Limitations of RF Ablation

Although RF ablation is a minimally invasive procedure, it has one limitation: the power supply is not optimized for the formation of an adequate ablation area. Several studies have investigated power supply methods, but they have not determined an optimal method for the formation of an adequate and suitable ablation area [1], [2]. Thus, it is difficult to control the coagulation zones precisely; tumors may recur in areas that have not been fully cauterized, and there is also the risk of burning the organs around the liver.

B. Controlling the Temperature of the Liver

Several studies have investigated temperature control in RF ablation. Chao et al. proposed an RF treatment system that used a fuzzy control algorithm to control the temperature of the RF trocar [3]. Haemmerich et al. developed multiprong type electrodes that can control the maximum temperature of the hepatic tissue [4]. Although these studies have the advantage of functionality to control the temperature of the tissue near the needle, they are not suitable for control of the tissue temperature away from the needle, as we intend. Kruse et al. presented a system to control the tissue temperature using proportional-differential-integral control [5]. However, this system increases the invasiveness by inserting a thermocouple. In contrast, there is a non-invasive method for sensing and monitoring of the temperature using magnetic resonance imaging (MRI) based on the temperature dependence of the phase difference of the protons in the tissue. However, MRI-based temperature-sensing methods have problems in that the sensed temperature accuracy is insufficient and the system itself is too large [6]. Therefore, there is a need for a method to sense the tissue temperature away from the electrode needle with low invasiveness and high accuracy.

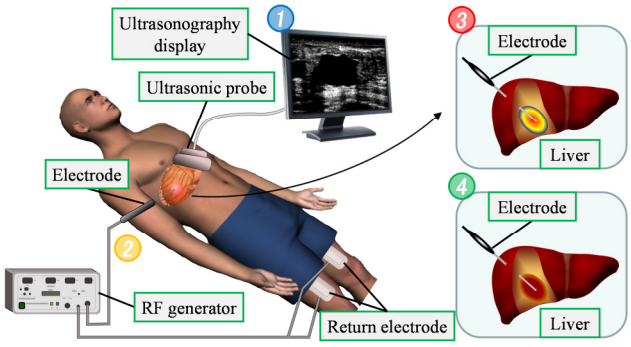

Figure 1. Liver RF ablation.

978-1-4577-0216-7/13/$26.00 ©2013 IEEE

C. Proposed System

To address the shortcomings of RF ablation, we propose a robot-assisted RF ablation system that can ensure an appropriately sized coagulation zone that conforms to the size of the targeted tumor. Our proposed system is shown in Fig. 2. This system can control the temperature of the tissue away from the electrode needle as required by the operator. Our approach uses a highly accurate temperature distribution simulator that we developed for this system, which can calculate the tissue temperature distribution. We have already reported the use of our temperature distribution simulator based on the precise thermophysical properties of a swine liver model while considering the cooling effect of the tissue blood flow [7], [8]. Using this simulator, the temperature of the liver away from the electrode needle can be estimated without increased invasiveness or additional device requirements. However, the temperature estimated by the temperature distribution simulator is not always the same as the temperature of a real liver ablation, because the thermophysical properties of the liver are different for each patient. Therefore, we used the temperature measured at the electrode needle as an indicator to enable us to calculate the temperature distribution around the electrode needle accurately using the temperature distribution simulator. The temperature of the electrode needle can be measured using a thermocouple implanted in the electrode needle. If the calculated electrode needle temperature is different to the measured temperature, then the accuracy of the simulation can be improved by modifying the thermophysical properties used in the simulation. The main problem with this control system is that it takes a long time to estimate the temperature distribution. The temperature estimation calculation must be complete to use this system in real time; therefore, we must find the lowest frequency of temperature calculation that will not reduce the control accuracy.

D. Objectives

The novelty of this study is the proposal and validation of a new system that can generate a coagulation zone that is appropriately sized relative to the dimensions of the tumor. Our investigations aimed to determine the appropriate time interval required to calculate the temperature distribution and thus control the size of the coagulation zones. The study uses the finite element method (FEM) for simulation of the system.

This report is organized as follows. Section II presents the numerical simulation and the algorithm of the proposed system. Section III presents an experiment using an agar phantom to validate the simulation. Section IV presents the results of the simulations and experiments, which are then discussed in Section V. Finally, Section VI presents our conclusions and plans for future work.

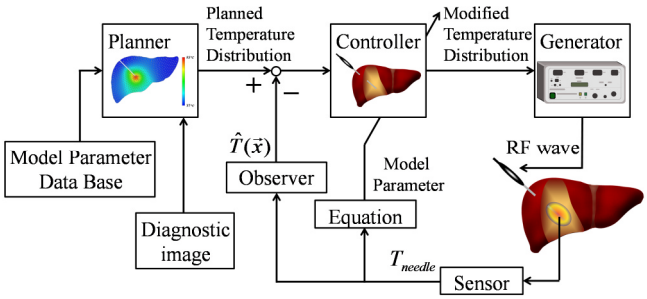

Figure 2. Temperature control system for liver RF ablation.

II. SIMULATION

We performed a numerical simulation to examine the effects of differences in the time taken to calculate the temperature in the temperature control system. We developed a three-dimensional temperature distribution simulator that can calculate the temperature distribution in liver tissue during RF ablation using the FEM. In the simulation, the heat generation is calculated using Laplace's equation (1) and Joule's law (2). The temperature distribution is then calculated using the Pennes bioheat equation (3) [9].

$$\nabla^2 \phi = 0, \tag{1}$$

$$Q = \sigma \left| \vec{E} \right|^2, \tag{2}$$

$$\rho c \frac{\partial T}{\partial t} = \lambda \nabla^2 T + Q - h(T - T_b), \tag{3}$$

where ϕ is the voltage (V), Q is heat generation (W/m^3), σ is the electrical conductivity of the organ (S/m), ρ is the density of the organ (kg/m^3), c is the specific heat of the organ (J/kgK), T is the temperature of the organ (°C), λ is the thermal conductivity of the organ (W/mK), h is the blood flow rate of the organ (W/m^{3}K), and T_b is the temperature of the blood (°C).

A. Conditions

Fig. 3 shows the simulation model, which has dimensions of 60 mm×60 mm×60 mm. The model contains one electrode needle inserted from the top surface of the model into the center of the model. The numbers of elements and nodes are 21,610 and 4,426, respectively. The source voltage V_{needle} (V) was applied to the conducting area of the RF electrode, which was the area within 20 mm of the head of the needle. The value of V_{needle} was changed in each cycle of the simulation to realize feedback control. The rest of the needle surface was considered to be non-conducting. At the bottom surfaces of the model, an electrical boundary condition of 0 V was applied to simulate the return ground electrode. An initial thermal condition of 33°C was applied for all elements, and the thermal boundary condition for the surface of the square was also set at 33°C. The thermal boundary conditions for the

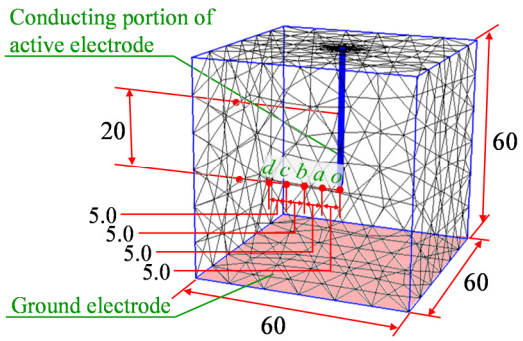

Figure 3. Simulation model.

electrode surface were again set to 33°C, assuming that hot water was flowing inside the electrode needle. The temperature was then measured at the four points *a*–*d*, situated 5-20 mm from the head of the needle.

B. Physical Properties

To compare the temperature obtained from the simulation with the results of the measurements described in Section III, we set the actual physical properties of the living body-equivalent agar phantom given in Table 1 as the parameters for the simulation model. We have previously measured the thermal and electrical conductivities of an isolated hog liver [10], and we confirmed here that these values for the agar phantom are close to those of the isolated hog liver.

C. Control Algorithm

The purpose of the present study is to determine an adequate time interval for feedback control. Therefore, to investigate the effect of the time interval only, we adopted proportional control of the output voltage with respect to temperature. In feedback control, the output voltage is calculated according to (4)–(10), as shown below.

$$V_{needle}(F_t k+1)=0\,, \tag{4}$$

$$\left(T_{target} < T_b(F_t k)\right), \tag{5}$$

$$V_{needle}(F_t k+1)=K_p\left[T_{target}-T_b(F_t k)\right]\,, \tag{6}$$

$$\left(T_b(F_t k)<T_{target}\ and\ K_p\left[T_{target}-T_b(F_t k)\right]<V_{\max}\right)\,, \tag{7}$$

$$V_{needle}(F_t k+1)=V_{\max}\quad, \tag{8}$$

$$\left(V_{\max}\le K_p\left[T_{target}-T_b(F_t k)\right]\right)\,, \tag{9}$$

$$\begin{aligned} &V_{needle}(F_t k+1)=V_{needle}(F_t k+2)=\ldots \\ &=V_{needle}(F_t k+F_t) \end{aligned}\,, \tag{10}$$

where V_{needle} is the electrode needle voltage (V), T_b is the temperature at point *b* calculated by the simulator (°C), K_p is the proportional gain, T_{target} is the target temperature at point *b* (°C), V_{max} is the maximum electrode needle voltage (V), F_t is the time interval taken to calculate T_b (s), and *k* is the number of calculation steps.

We decided to control the temperature at point *b*, which is 10 mm from the electrode needle when considering the ablation of a 20 mm sized tumor. We set T_{target} to 60°C as the temperature at which coagulation occurs. Fig. 4 shows the execution flow of the simulation. In the simulation, numerical calculations are performed repeatedly. We set the actual time per calculation step to 1.0 s and ran the calculation for 900 steps. The total actual calculation time is thus 900 seconds. The value of V_{needle} is changed at intervals of F_t in the simulation to realize feedback control. This means that the temperature at *b* is estimated once per F_t. There are, however, restrictions on the changes in V_{needle}. First, V_{needle} cannot be negative, and V_{needle} is thus set to 0 V when T_b exceeds T_{target}, according to (4) and (5). V_{needle} must also be less than V_{max},

TABLE I. MODEL PARAMETERS

Density ρ (kg/m^3)	997
Specific heat c (J/kgK)	4200
Thermal conductivity λ (W/mK)	0.67
Electrical conductivity σ (S/m)	0.0079T+0.1599 (T<90) 0.8709 (90<T)
Blood perfusion h (W/m^{3}K)	0

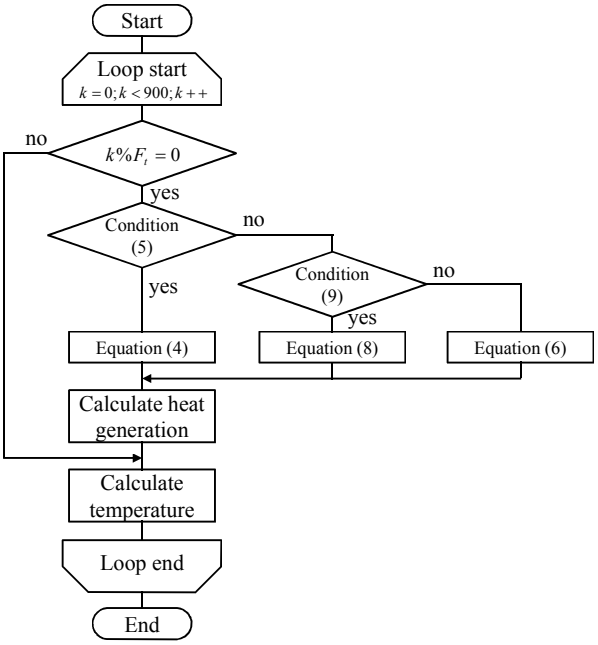

Figure 4. Simulation execution flow.

according to (8) and (9), because when the output is too large, the tissue around the electrode is carbonized, which makes proper treatment impossible. At this time, V_{max} is set to 40 V. Finally, V_{needle} maintains the same value for the duration of F_t, according to (10). We use a proportional gain of 15, for which there is both a small temperature fluctuation and a small steady-state deviation.

D. Results

Fig. 5 shows the simulation results for a time interval of 5 s, as an example of the results for all conditions. The figure shows a cross-sectional view of the model with a portion removed to see the internal temperature distribution. It is shown that the temperature increases around the needle.

Fig. 6 shows the simulated temperature and voltage for time intervals F_t of 5 s and 30 s. The temperature fluctuation tendencies are highly similar at points *b*-*c*. When the time interval is small, the control is stable and V_{needle} quickly converges to a constant voltage. In contrast, the output

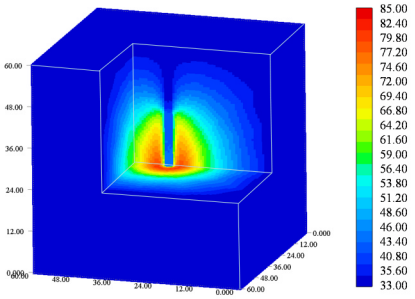

Figure 5. Simulation results.

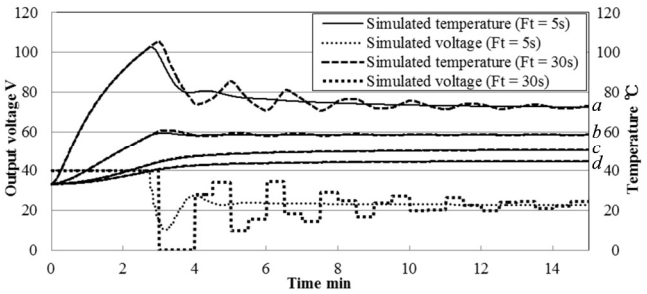

Figure 6. Simulated temperature and voltage values.

voltage fluctuation is no longer smooth when the time interval is large. As a result, when the time interval is large, the temperature fluctuation is also large, and there is therefore a delay in convergence, especially at point *a*.

The simulation is tested on a PC with Intel Core i7 3.4 GHz CPU and 4 GB RAM. It takes approximately 24 second per calculation step and additional 10 second when the value of V_{needle} is changed.

III. EXPERIMENTAL

To evaluate the validity of the simulation results, we conducted an experiment using an agar phantom.

A. Conditions

Fig. 7 shows the experimental setup. We cauterized an agar phantom using a Cool-tip RF system under the same physical conditions as those used in the simulations described in Section II. The phantom was made from 4% agar, 0.3% NaCl and water. The phantom was situated in a temperature-controlled bath so that all of its surfaces were controlled to a constant temperature. We set the temperature-controled bath to 37°C. However the results show that the actual temperature was 33°C. The lower surface of the phantom was in contact with a return electrode that absorbed the RF current flow from the active electrode. Hot water heated by the temperature-controlled bath was flown inside the needle type active electrode by a pump so that the phantom did not become too hot.

B. Method

Fig. 8 shows a diagram of the temperature control system. Rather than estimate the temperature of the phantom away from the electrode needle, we used a thermocouple and measured the temperature. Using the temperature at point *b*, the output voltage (V_{needle}) is decided by the algorithm given in (4)–(10). The output dial is rotated to control the output voltage through a servomotor, based on feedback control by comparing V_{needle} and the current voltage ($V_{current}$). Therefor the amplitude of the pulse can be controlled. Using these devices, we carried out the ablation experiments as follows. 1) First, the temperature of the phantom was controlled to 33°C by the hot water. 2) After the temperature of the phantom reached the target temperature, the needle type active electrode and four thermocouples were then inserted into the phantom. 3) V_{needle} was applied to the phantom via the active electrode, and the temperatures were measured at the four points *a*–*d* during ablation.

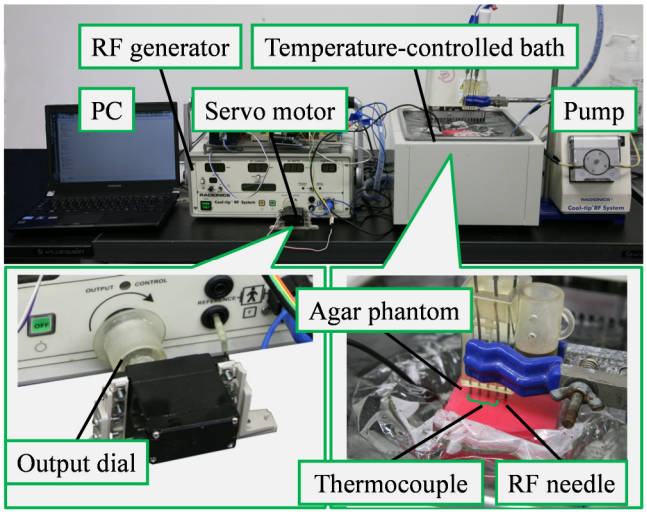

Figure 7. Experimental setup for cauterization of agar phantom using temperature control system.

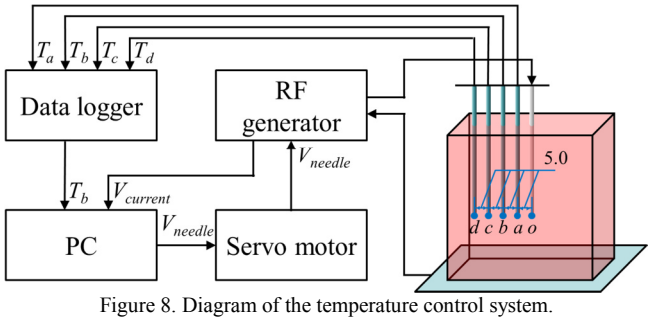

Figure 8. Diagram of the temperature control system.

IV. RESULTS

Figs. 9-10 show comparisons of the results of the simulations and the experiments. The temperature fluctuation tendencies are very similar for the simulations and experiments at points *b*-*c* for both time intervals of 5 s and 30 s.

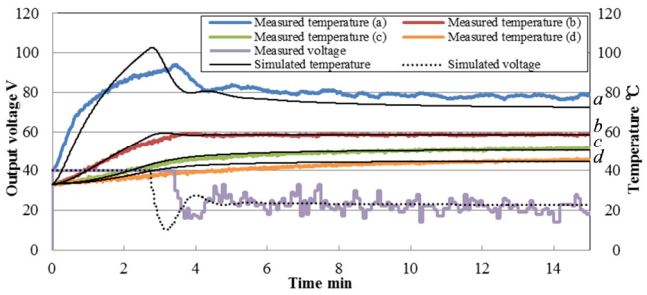

Figure 9. Comparison of the results of simulations and experiments at time intervals of 5 s.

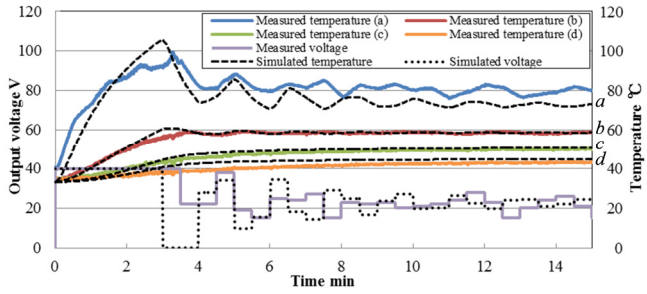

Figure 10. Comparison of the results of simulations and experiments at time intervals of 30 s

V. DISCUSSION

In RF ablation, if the output voltage is changed frequently, then the control will be stable. However, it is necessary to change the output voltage at appropriate intervals for real time control. Because the point at which we need to control the temperature is away from the electrode needle, and it is thus difficult to measure the temperature at this point, we used our proposed method to estimate the temperature by simulation, which takes a long time. In the method, the time intervals used for the change in output voltage and the temperature estimation are the same. Therefore, to realize temperature feedback control using our method, it is important to use the longest possible time interval that allows stable control of the system. We thus evaluated the relationship between the time interval F_t and the control stability by numerical simulation, and we conducted experiments using the agar phantom to evaluate the validity of the simulation results.

First, we discuss the accuracy of simulation results. The temperature fluctuation tendencies are very similar in the simulations and experiments at points *b*-*c* for both time intervals of 5 s and 30 s (see Figs. 9–10). However, the temperature at point *b* reached 60°C earlier in the simulations than in the experiments. To explain this result, we focus on the temperature fluctuation at point *a*. The slope of the temperature fluctuation at point *a* suddenly became small at around 70°C in the experiments. This is probably because when the temperature was close to 90°C, the phantom near the needle melted and the temperature conduction became small. Although water was flowing inside the electrode needle to avoid melting of the phantom, it was not enough. For these reasons, although there are some gaps between the results of the simulations and the experiments, the results coincide well after the control begins.

The results show that when the time interval is small, the control is stable and V_{needle} quickly converges to a constant voltage. In contrast, the output voltage fluctuation is no longer smooth when the time interval is large. As a result, when the time interval is large, the temperature fluctuation is also large, and there is a delay in convergence at point *a* near the head of the needle. However, the time interval had little effect at points *b*-*d* far from the head of the needle, and the results were almost same, regardless of the time interval. These results mean that it is necessary to reduce the time interval when small tumors are to be cauterized to avoid excessive treatment. In contrast, we do not have to reduce the time interval when large tumors are cauterized.

As shown above, it is possible to perform an accurate simulation even under complex conditions like water flowing inside the needle by making a precise model with consideration of the shapes and physical properties. We have shown that by controlling the output of the generator by using such a simulation, it is likely to be possible to control the temperature at points away from the electrode needle to obtain the desired ablation size.

VI. CONCLUSION

We proposed a new system for temperature control away from the electrode needle during RF ablation using FEM simulation. We evaluated the relationship between the time interval, the change in the output voltage and the temperature control stability in RF ablation. The results show that it is likely to be possible to control the temperature at points away from the electrode needle by using such simulations and controlling the generator output. It was found that it is necessary to reduce the time interval when small tumors are cauterized to avoid excessive treatment, but we do not have to reduce the time interval when large tumors are cauterized.

When the system is used in clinical practice, the time taken to perform the calculation will depend on the differences between individual patients, the accuracy of the model and the power of the computers used. The time interval obtained in this study can be used as a guide to determine the configuration of a system for use in clinical practice. In vitro and in vivo experiments must be performed in future work to validate the proposed method.

REFERENCES

[1] J. P. McGahan, S. Loh, F. J. Boschini, E. E. Paoli, J. M. Brock, W. L. Monsky and C. S. Li, "Maximizing parameters for tissue ablation by using an internally cooled electrode," *Radiol.*, vol. 256, pp. 397-405, Aug. 2010.

[2] M. K. Jain and P. D. Wolf, "Temperature-controlled and constant-power radio-frequency ablation: what affects lesion growth?" *IEEE Trans. Biomed. Eng.*, vol. 46, pp. 1405-1412, Dec. 1999.

[3] C. Meng, W. Sun, Y. Chen, Y. Li and L. Liu, "Application of temperature fuzzy control system in RF treatment for nerve ache," in *Proc. 6th Int. Conf. FSKD Conf. Fuzzy Systems and Knowledge Discovery*, 2009, pp. 62-65.

[4] D. Haemmerich, S. Tungjitkusolmun, S. T. Staelin, F. T. Lee, Jr., D. M. Mahvi, and J. G. Webster, "Finite-element analysis of hepatic multiple probe radio-frequency ablation," *IEEE Trans. Biomed. Eng.*, vol. 49, pp. 836-842, 2002.

[5] D. E. Kruse, Chun-Yen Lai, D. N. Stephens, P. Sutcliffe, E. E. Paoli, S. H. Barnes and K. W. Ferrara, "Spatial and Temporal-Controlled Tissue Heating on a Modified Clinical Ultrasound Scanner for Generating Mild Hyperthermia in Tumors," *IEEE Trans. Biomed. Eng.*, vol. 57, pp. 155-166, 2010.

[6] M. Lepetit-Coiffe, H. Laumonier, O. Seror, B. Quesson, M. B. Sesay, C. T. Moonen, N. Grenier and H. Trillaud, "Real-time monitoring of radiofrequency ablation of liver tumors using thermal-dose calculation by MR temperature imaging: initial results in nine patients, including follow-up," *Eur. Radiol.*, vol. 20, pp. 193-201, Jan. 2010.

[7] H. Watanabe, N. Yamazaki, Y. Kobayashi, T. Miyashita, M. Hashizume and M. G. Fujie, "Temperature dependence of thermal conductivity of liver based on various experiments and a numerical simulation for RF ablation," in *Proc. 32rd Ann. Int. Conf. IEEE Engin.. Med. Biol. Soc.*, pp. 3222-3228, 2010.

[8] H. Watanabe, N. Yamazaki, Y. Kobayashi, T. Miyashita, M. Hashizume, M. G. Fujie, "Estimation of Intraoperative Blood Flow During Liver RF Ablation Using a Finite Element Method-based Biomechanical Simulation", in *Proc. 34rd Ann. Int. Conf. IEEE Engin. Med. Biol. Soc.*, pp. 7441-7445, 2011.

[9] H. H. Pennes, "Analysis of tissue and arterial blood temperatures in the resting human forearm", *J. Appl. Physiol.*, vol. 1, no. 2, pp. 93–122, 1948.

[10] H. Watanabe, N. Yamazaki, Y. Kobayashi, T. Miyashita, M. Hashizume, M. G. Fujie, "Validation of Accuracy of Liver Model with Temperature-Dependent Thermal Conductivity by Comparing the Simulation and in vitro RF Ablation Experiment", in *Proc. 34rd Ann. Int. Conf. IEEE Engin. Med. Biol. Soc.*, pp. 5712-5717, 2012.